

Microstructure and electrical resistivity features in Al-Al₄C₃ in-situ composite after attrition milling and double sequence of compaction and high temperature treatment

A. T. Özdemir*, B. Bostan

Gazi University, Faculty of Technology, Department of Materials and Metallurgical Engineering, Ankara, Turkey

Received 10 July 2011, received in revised form 30 July 2011, accepted 17 August 2011

Abstract

An Al-based composite powder (Al-2%C) was prepared by mechanical alloying (MA). Mixed powders were cold compacted and annealed using two consecutive treatments. Microstructure progresses in both; the as-milled and the as-pressed and annealed conditions were characterized by X-ray diffractometry (XRD) and transmission electron microscopy (TEM). During MA, C diffused into Al to form a solid solution. However, for MA, primary compaction and 1 h sintering at 650 °C was insufficient to synthesize Al with C. Only after secondary pressing and long-time annealing at 550 °C, fine precipitates of Al₄C₃ were formed throughout the matrix. Increase in Al₄C₃ dispersion and stabilization of a dense dislocation substructure was the main source of systematic rise in both electric resistivity and hardness.

Key words: mechanical alloying, synthesizing, Al₄C₃ precipitation, electrical resistivity

1. Introduction

Design and manufacture of modern materials for application in aerospace and defense industries are gaining importance. To prepare stronger and heat resistant but lighter multifunctional materials, modifications both in chemical and physical properties as well as advanced heat, mechanical and thermo-mechanical treatments are essential [1]. In high temperature technology, creep resistance specially requires additional strengthening through fine particles of the minor phase finely dispersed in the matrix. This phase either represents a product of decomposition of the matrix solid solution or is introduced into the matrix by a special powder metallurgy (PM) technique as dispersion strengthened alloys.

As a part of PM, mechanical alloying (MA) was first introduced to control the size, volume percent and homogeneous distribution of fine hard oxide and inter-metallic particles to optimize the strength of superalloys with the concept of metal matrix composites (MMCs) [2–6]. Through recent developments in this technique, manufacturing of amorphous [7, 8] and intermetallic materials [9] have gained further interest.

Method of MA mainly involves a *high energy attritor* in which steel or ceramic ball are used to blend metal powders at desired proportions by successive crushing and welding of metal powders through the process [10, 11]. MMCs manufactured by MA can keep their high strength properties close to melting point [12] together with good corrosion resistance [13, 14]. Because of the rapid progress, MA method seems promising in developing new Al-based composites. However, reactive nature of fine Al powders requires new procedures of processing and equipment to prevent contamination and explosion [15]. Recent researches reveal that addition of fine oxides and carbides can contribute to high temperature strength together with advanced toughness, fatigue and corrosion properties [16]. Some preliminary studies were concentrated on *in-situ* Al composites reinforced by fine Al₄C₃ and Al₂O₃ precipitates, where results reveal these particles have considerable effects on optimum mechanical properties of the materials [17–25]. In several alloy systems, synthesizing of these stable precipitates through MA process is gaining interest in the last decade. Contrary to the early promise, development is slow, and the major progress of the method is: the alloy development, modi-

*Corresponding author: tel.: 903122028755; fax: 903122120059; e-mail address: 2007atam@gmail.com

fication of powder characteristics and optimization of novel manufacturing processes.

In this study, experiments have been conducted on a laboratory scale to investigate the characteristics of blended Al-C powders and the effect of multiple pressing and annealing on the formation of Al_4C_3 phase dispersion and its consequential effect on the electrical resistivity and hardness values of the composite material.

2. Experimental

Powders were commercial grade atomized 99 % pure Al supplied from Aldrich and 99.9 % pure C from Alfa Aesar, where the sizes were under -200 mesh and between -20 , $+84$ mesh, respectively. Al-2%C powders by weight were mixed and then placed in a gas tight, water cooled horizontal high energy attritor for high speed ball milling. A gas purifying furnace containing copper scraps at 475°C was also connected to the system. During attrition, powder/steel ball ratio was 1 : 20 and optimum speed of the attritor was about 600 rev min^{-1} .

To resolve the effect of processing time on the performance of MA, powders were treated for 1 and 2 h, where the milling process was interrupted at quoted time intervals and small samples of as-milled powders were taken out to exemplify the mixture characteristics. Thus, a Malvern Mastersizer E laser light scattering machine and a Rigaku Geigerflex X-ray diffractometer (XRD) with $\text{Cu K}\alpha$ radiation were used to verify the size distribution and the formation of the Al_4C_3 phase in the powder mix. After MA, small samples of blended powders (about 1 g) were cold pressed into small discs under a pressure of 1200 MPa and then sintered at 650°C for 1 h (primary treatment). To study the structural variation, discs were subsequently repressed under 600 MPa and then annealed at 550°C for 2–32 h (secondary treatment). Each heat treatment cycle was completed in flowing purified argon gas. To identify the formation and morphology of Al_4C_3 precipitates, a Jeol 3010 transmission electron microscope (TEM) at an accelerating voltage of 300 kV was used. Thin foil disc specimens of 3 mm for TEM were prepared by a conventional Struers Tunepol-3 electropolishing unit with a solution of perchloric acid (10 vol.%), glycerol (20 vol.%) and methyl alcohol (70 vol.%). In order to avoid any possible chemical interaction between the electrolyte and the precipitates, foil discs were further thinned to perforation by gentle jet polishing at -40°C , where the applied current of $30 \mu\text{A}$ with $5 \text{ cm}^3 \text{ s}^{-1}$ of flow rate was a standard for thin foil preparation. Hardness values of the samples were measured by using a Vickers hardness tester under 1 kg force, where at least 20 measurements randomly from the surface of each

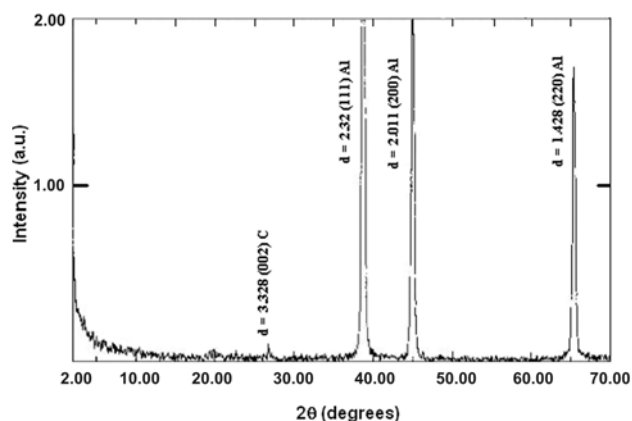


Fig. 1. XRD of blended Al-C powders after 1 h MA.

specimen were taken. Finally, electrical resistivity values of the compacts having thickness of 1 mm were measured at room temperature using a 22 A Keitley instrument with a high sensitivity manipulator.

3. Results and discussion

3.1. Mechanical alloying

Al and C powders were used as-received to synthesize the Al_4C_3 phase in pure Al. The typical sizes of original Al and C powders were about $110 \mu\text{m}$ and $150 \mu\text{m}$ in diameter, respectively. At the beginning of MA, Al powders were rapidly and concurrently flattened, crushed, cold-welded and so strain-hardened. Meanwhile, soft free C was squeezed, pulverized and spread over the coarse elongated lamellae structure of Al resulting in a coarse convoluted lamellae structure, where after 1 h MA particle size was about $52.85 \mu\text{m}$. By the further milling, powder microstructure thoroughly was refined and homogenized. At the end of 2 h MA, both mean particle size ($18.58 \mu\text{m}$) and lamellae spacing became smaller (less than $3 \mu\text{m}$ in size). At this stage, free C dust possibly extruded in and coated the interface of the multilayered lamellae structure [21, 22]. Further attempts to increase the attrition time failed, because mean Al powders size became less than $10 \mu\text{m}$ and so the flammability of these fine Al dusts increased intensively.

To determine the effect of MA, composite powders were analyzed by XRD. Prior to MA, powder mix had a strong line of (002) peak for free C. After 1 h MA, this peak partially weakened and near by 2 h MA, vanished completely (Figs. 1 and 2). The absence of C peak was an evidence of refining and dissolving of graphite in Al to form a solid solution at the end of MA. By elemental diffusion, atomic C penetrated in and located at interstitial sites of the convoluted crys-

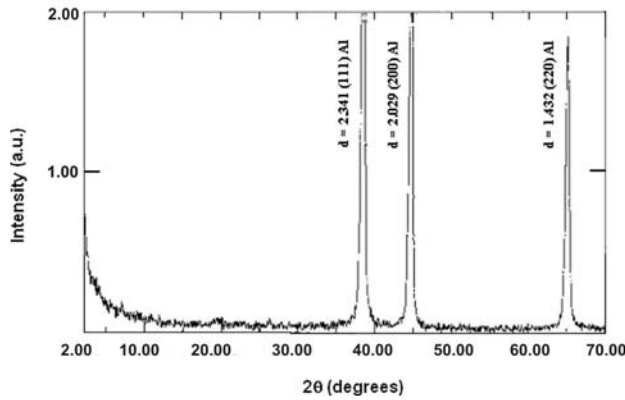


Fig. 2. XRD of blended Al-C powders after 2 h MA.

tal structure of Al. This was either due to very short milling time resulting inadequate synthesizing time for the formation of the Al_4C_3 phase [19–22, 26] or due to the amorphous phase of Al_4C_3 that formed before crystallization [20, 27, 28]. Consequently, development of Al_4C_3 was thermodynamically impractical during MA [28].

3.2. Duplex treatment

In this work, to evaluate the effect of the consolidation pressure intensity on Al_4C_3 precipitation, cold pressing was accomplished in two consecutive steps. After cold pressing under 1200 MPa and primary annealing at 650 °C (primary treatment), the compacts were repressed under 600 MPa pressure and subjected to secondary annealing at 550 °C (secondary treatment). The aim was to induce more energy in order to increase the driving force to transform C into Al_4C_3 . Formation of a dense dislocation substructure was expected to stimulate the precipitation Al_4C_3 phase on many potential nucleation sites [29].

Microstructural evolution during secondary annealing was investigated by TEM. A bright field image at low magnification shows the distribution of the clusters of Al_4C_3 precipitates (Fig. 3). The selected area diffraction pattern (SADP) of the same area is shown in Fig. 4. There are numerous diffraction spots of the Al_4C_3 phase evenly distributed on the continuous rings of the f.c.c. structure. Dark field image of (0012) reflection with very small objective aperture (diameter 5 μm) clearly allows separating the Al_4C_3 phase diffraction from that of the Al_2O_3 phase. Precipitates are very small in size and most often are in groups or clusters. At high magnifications, a close up dark field examination indicates that in each Al_4C_3 cluster, individual precipitates are closely spaced (Fig. 5) and mostly settled on the dislocation substructure of Al (Fig. 6). Depending on the orientation, precipitates are mostly disc like. On the average,

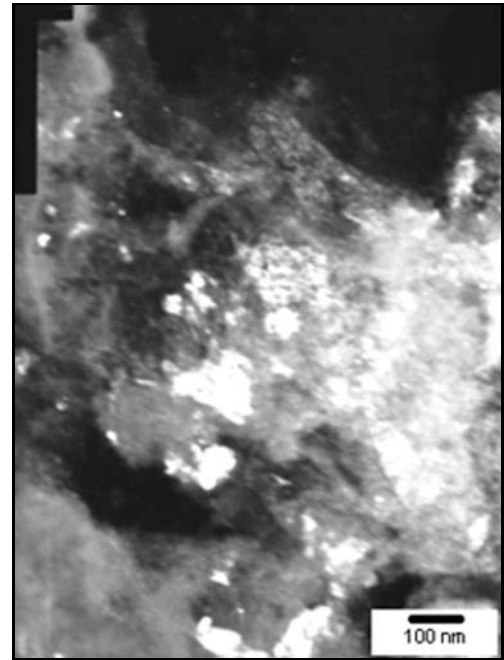


Fig. 3. TEM dark field image of (0012) plane reflection at low magnification after secondary annealing at 550 °C for 32 h, showing distribution of dense clusters of Al_4C_3 precipitates.

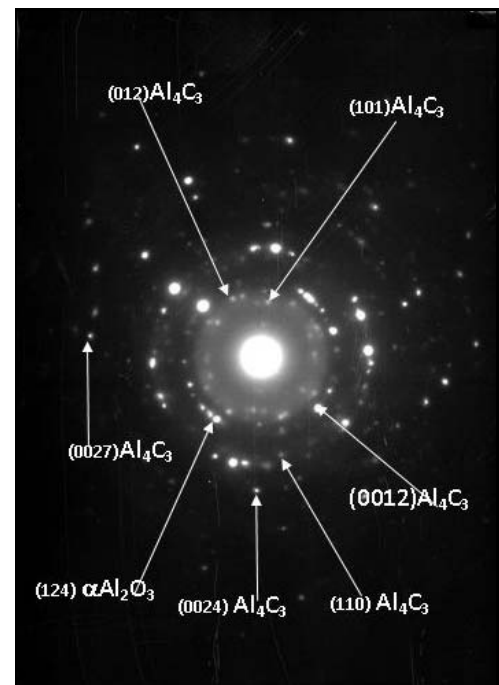


Fig. 4. SADP of the region shown in bright field.

they have thickness, T , of 1.4 nm, length, L , of 4 nm and width, W , of 1.8 nm, respectively, where the mean aspect ratio, L/W , of the precipitates is around 2.2.

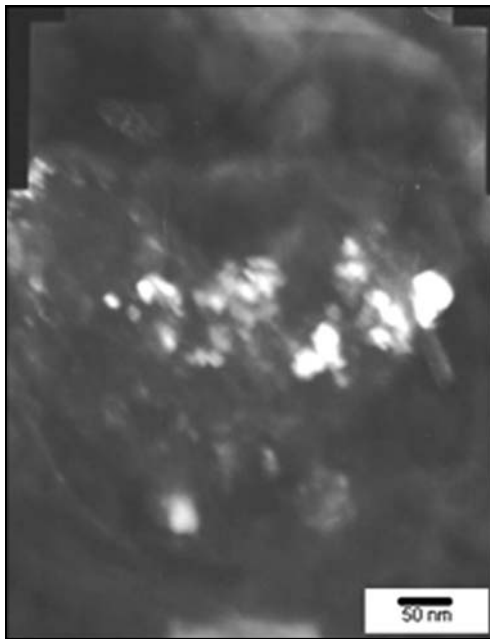


Fig. 5. TEM micrograph at high magnification illustrating dark field image of (101) plane reflection, showing individual Al_4C_3 precipitates within clusters.

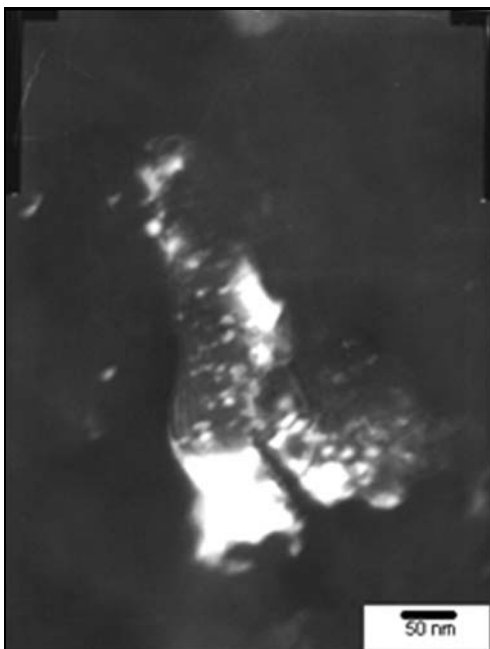


Fig. 6. TEM dark field image of (101) plane reflection at high magnification, showing Al_4C_3 precipitates settled on a substructure.

The average cluster size is 39 nm and mean spacing between the clusters is 118 nm. Thus, compared to previous work [21, 22], precipitates are finer and more closely spaced.

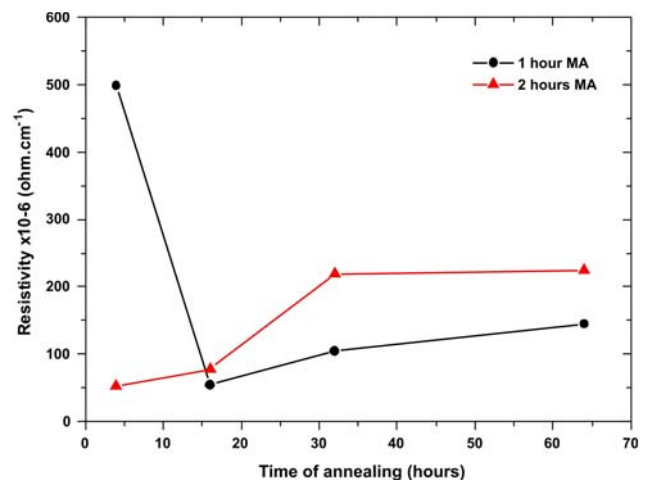


Fig. 7. Change in electrical resistivity with respect to MA time and duration of secondary annealing at 550°C.

3.3. Electrical resistivity

Electrical resistivity is sensitive to numerous microstructural factors. It is correlated to lattice defects and imperfections, such as vacancies and solute concentrations, and in case of precipitation, to the precipitate or cluster (pre-precipitate) size and volume fraction [30]. It is clear that MA is very effective in controlling the size, volume percent, distribution of the added particles, and so homogenization of the microstructure. However, during MA the density of lattice defects and imperfections inevitably aggravates. Thus, electrical resistivity is naturally expected to increase progressively during the process [30, 31].

In the present work, after the secondary compaction cycle but before the secondary annealing at 550°C, resistivity values for 1 and 2 h MA were measured as 498 and 53 $\mu\Omega \text{cm}^{-1}$, respectively (Fig. 7). This result was contrary to the above anticipations. During MA, the amount of the admixed lubricant among Al powders dictated this change in resistivity measurements [32, 33]. The free C played an important role. After 1 h MA, excess C (Fig. 1) extruded out and occupied the pores, limiting the maximum available density even at high degree of compaction [32]. Due to lessening of metal to metal contacts (i.e., interparticular insulation), electrical resistivity was high. However, after 2 h MA mean powder size became smaller. Free C was almost absorbed in and so could not surround and insulate the Al powders. The measured resistivity value was therefore comparatively low (Fig. 2).

During secondary annealing and at the end of 16 h annealing, resistivity values were 55 and 78 $\mu\Omega \text{cm}^{-1}$ for 1 and 2 h of MA. On further annealing, resistivity increased and after 32 h, reached to 105 and 219 $\mu\Omega \text{cm}^{-1}$. Finally at the end of 64 h, resistivity values gradually became 145 and 225 $\mu\Omega \text{cm}^{-1}$, re-

spectively. This continuous rise in resistivity could not be due to the metallic contacts. Porosity, on the other hand, could not contribute to this variation in resistivity, because after primary and secondary annealing processes, the measured porosity values were close to 1.1 %. Therefore, the mechanism controlling electrical resistivity was altered. During secondary annealing at 550 °C, Al_4C_3 precipitation initiated where particles increased in number and started to act as the main factor controlling the changes in electrical resistivity.

In many conventional, age-hardenable Al alloys, introduction of even a single solute atom into the matrix will cause an incremental increase in electrical resistivity. Although a detailed picture of the operating microstructural mechanisms are said to be still ambiguous, increase in resistivity is mostly attributed to the formation of non-random precipitates [30, 31]. The maximum value occurs, when the zone reaches a critical size equal to the wave length of the conducting electrons. As such, the maximum corresponds with a definite zone size which varies from alloy to alloy. When a typical precipitate or cluster radius is less or within the order of the size of mean free path, resistivity increases to the peak value apparently.

There is in fact no detailed information about the precipitation sequence of the fine Al_4C_3 particles and its mutual interaction with electrical resistivity in Al. A little knowledge is that these neutral ceramic particles are very stable and resistant to ‘Ostwald Ripening’ during prolonged annealing [19] and they have significantly high room temperature self electrical resistivity values [34]. The information obtained with TEM technique through the previous [21, 22] and present works nevertheless draw attention, that rise in electrical resistivity of Al can be attributed to the increase in distribution and density of the Al_4C_3 precipitation in the matrix. Presumably, rather than the size and spacing of distinctive precipitates [19], the dimension of the non-random Al_4C_3 clusters and the spacing between them govern the electrical resistivity. Similar to age hardening Al alloys, they may involve in scattering and interfere with the mean free path of the electrons running in [30, 31].

3.4. Hardness

Change in microhardness with secondary annealing time is given in Fig. 8. Similar to electrical resistivity, at the beginning of annealing at 550 °C, hardness values are high. But after a short time, they reduce down. Reaching to a minimum, hardness values start to increase gradually. There is a great difference between the hardness profiles for 1 and 2 h MA before the onset of annealing. This variation is most likely as a result of remarkably refined powder size reached after 2 h MA. During secondary pressing, the compacted material is cold worked severely; in return the current

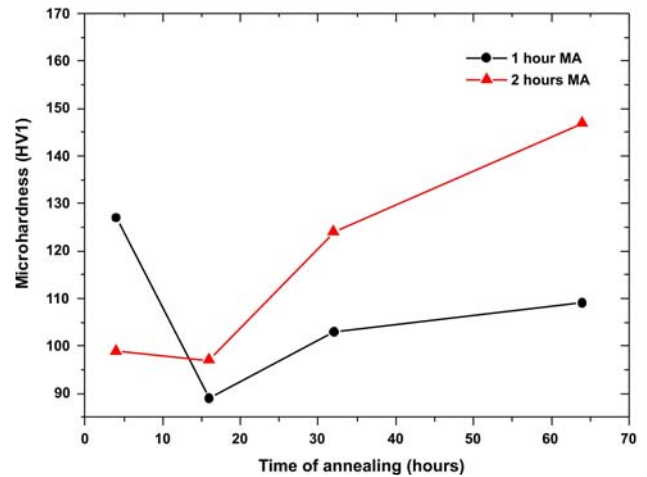


Fig. 8. Change in hardness with respect to MA time and duration of secondary annealing at 550 °C.

compacts made from finer powders achieve high hardness values. As seen from the figure, at the onset of secondary annealing the initial high hardness values reduce in magnitude. This fall in hardness is possibly due to strain softening and recovery mechanisms activated in the structure. As secondary annealing proceeds, steady elevation in hardness takes place, which is undoubtedly a result of rapid Al_4C_3 precipitation. The compacts of 2 h MA have higher hardness values than those of the compacts of 1 h MA. When compared to the hardness values of single pressed samples [21, 22], double pressed compacts on the average reach high hardness levels.

C dissolution in Al is a key factor. It is clear from the experiments that, C completely supersaturates in refined Al powders particularly after 2 h MA (Fig. 2). This in fact increases the potential to form a dense Al_4C_3 precipitation and cluster formation on the substructure of Al during the cycle of secondary treatment [26, 28, 29, 35]. Thus, more C dissolution means more potential and driving force for Al_4C_3 formation in Al.

C in Al has very low solubility limit (less than 10^{-4} wt.%) [36], so Al_4C_3 precipitates are very stable and fine in size [19]. Precipitation is presumably due to reduction in overall lattice strains, normally generated after severe cold working [29]. Small dissolved interstitial atoms customarily have a tendency to settle on the strain fields of dislocations. Early development of a dense dislocation substructure therefore promotes nucleation sites for heterogeneous precipitation [29, 35, 37, 38]. Al_4C_3 precipitates mostly settle on dislocation nodes and the average spacing between the precipitates is possibly within the order of the cell size in the substructure [38, 39]. Thus, the pressure of compaction controls the density of the dislocation substructure and Al_4C_3 precipitation stabilizes this sub-

structure. Consequently, formation and multiplication of fine Al_4C_3 precipitates increases both electrical resistivity and hardness of the material. For surviving at high temperatures, these fine Al_4C_3 precipitates have the tendency to withstand particle coarsening [19], and so softening of the material during prolonged annealing or exposure to high temperatures [40, 41].

4. Conclusions

1. During MA and 1 h annealing at 650 °C (primary treatment), Al_4C_3 phase could not be synthesized in Al-C mixture. Fine precipitates of Al_4C_3 could only be formed after double pressing and during secondary annealing at 550 °C (secondary treatment).

2. Al_4C_3 precipitates are mostly in clusters and heterogeneously sited on the pre-created dislocation network arrays of the heavily cold-worked substructure generated after double pressing. When secondary annealing time proceeds, the size and the population of the precipitates or clusters increase. In return, electrical resistivity and hardness of the compacts rise progressively.

3. Changes in electrical resistivity and hardness are in good agreement, where a parallelism exists between them. It is unambiguous that electrical resistivity measurements can be useful in studying the precipitation sequence of Al_4C_3 phase and the microstructural changes within the material.

References

- [1] BLOOR, D.—BROOK, R. J.—FLEMINGS, M. C.—MAHAJAN, S. M.: The Encyclopedia of Materials. Oxford, Pergamon Press 1999.
- [2] SURYANARAYANA, C.: Proc. Mater. Sci., 46, 2001.
- [3] ARZT, E.: In: Proceedings New Materials by Mechanical Alloying Techniques. Eds.: Arzt, E., Schultz, L. Oberursel, DGM Germany 1988, p. 185.
- [4] HENDRICH, H. D.: In: Proceedings New Materials by Mechanical Alloying Techniques. Eds.: Arzt, E., Schultz, L. Oberursel, DGM Germany 1988, p. 217.
- [5] BENJAMIN, J. S.—BOMFORD, M. J.: Met. Trans., 8A, 1977, p. 1301.
- [6] BENJAMIN, J. S.—SCHELLENY, R. D.: Met. Trans., 12, 1981, p. 1827.
<http://dx.doi.org/10.1007/BF02643766>
- [7] KOBAYASHI, K. F.—TACHIBANA, N.—SHINGU, P. H.: J. Mater. Sci., 25, 1983, p. 3149.
<http://dx.doi.org/10.1007/BF00587665>
- [8] KOCH, C. C.—CAVIN, O. B.—McKAMEY, C. G.—SCABROUGH, J. O.: Appl. Phys. Lett., 43, 1983, 1017. <http://dx.doi.org/10.1063/1.94213>
- [9] FAIR, G. H.—WOOD, J. U.: Powder Met., 36, 1983, p. 123.
- [10] HAUSER, H. H.—SMITH, W. E.: Metal Powder Int. Fed., 6, 1973, p. 1.
<http://dx.doi.org/10.2497/jispm.6.1>
- [11] KOCH, C. C.: Annu. Rev. Mater. Sci., 1, 1970, p. 2943.
- [12] RUHLE, M.—KARLO, G.: In: Proceedings Novel ODS Superalloys Manufacture and Properties Heat Resistant Materials. Ed.: Bhushan, B. Fontana, Wisconsin, CRN Press USA 1991, p. 45.
- [13] TYONG, J. C.—MA, Z. Y.: Mater. Sci. Eng. Reports, 29, 2000, p. 49.
[http://dx.doi.org/10.1016/S0927-796X\(00\)00024-3](http://dx.doi.org/10.1016/S0927-796X(00)00024-3)
- [14] GUTMANAS, E. Y.: In: Proceedings New Materials by Mechanical Alloying Techniques. Eds.: Arzt, E., Schultz, L. Oberursel, DGM Germany 1988, p. 129.
- [15] JANGG, G.—SLESAR, M.—BESTERCI, M.—DURISIN, J.—SCHRODER, K.: Pow. Met. Int., 21, 1989, p. 25.
- [16] BESTERCI, M.—SLESAR, M.—KOVAC, L.: Scripta Mater., 37, 1997, p. 1077.
- [17] BARLOW, I. C.—JONES, H.—RAINFORTH, W. M.: Scripta Mater., 44, 2001, p. 79.
- [18] BESTERCI, M.—IVAN, J.—KOVAC, L.: Mater. Sci. Forum, 1–3, 2001, p. 1469.
- [19] BESTERCI, M.: Mater. Design, 27, 2006, p. 416.
- [20] ZHOU, Y.—LI, Z. Q.: J. Alloys Compd., 414, 2006, p. 107. <http://dx.doi.org/10.1016/j.jallcom.2005.07.034>
- [21] ÖZDEMİR, A. T.: Synthesizing of Aluminium with Carbon. Technical Report (BAP-07/2002-05). Ankara, Turkey, Gazi University 2002.
- [22] BOSTAN, B.—ÖZDEMİR A. T.—KALKANLI, A.: Powder Metall., 47, 2004, p. 37.
<http://dx.doi.org/10.1179/003258904225015400>
- [23] BELTRAN, A. S.—OROZCO, V. G.—GUEL, I. E.—GOMEZ, L. B.—MAGANA, F. E.—YOSHIDA, M. M.—SANCHEZ, R. M.: J. Alloys Compd., 434–435, 2007, p. 514.
<http://dx.doi.org/10.1016/j.jallcom.2006.08.303>
- [24] REYES, R. G.—OROZCO, V. G.—ZUNIGA, H. F.—HERNANDEZ, F. A.—ACUNA, R. H.—SANCHEZ, R. M.—BELTRAN, A. S.: J. Alloys Compd., 485, 2009, p. 837.
<http://dx.doi.org/10.1016/j.jallcom.2009.06.105>
- [25] GUEL, I. E.—GALLARDO, C. C.—RUIZ, D. C. M.—YOSHIDA, M. M.—RANGEL, E. R.—SANCHEZ, R. M.: J. Alloys Compd., 483, 2009, p. 173.
<http://dx.doi.org/10.1016/j.jallcom.2008.07.190>
- [26] MAURICE, D. R.—COURTNEY, T. H.: Metall. Trans., 21A, 1990, p. 289.
- [27] SINGER, R. F.—OLIVER, W. C.—NIX, W. D.: Metall. Trans., 11A, 1980, p. 1895.
- [28] WU, N. Q.—WU, J. M.—WANG, G. X.—LI, Z. Z.: J. Alloys Compd., 260, 1997, p. 121.
[http://dx.doi.org/10.1016/S0925-8388\(97\)00138-2](http://dx.doi.org/10.1016/S0925-8388(97)00138-2)
- [29] MARTIN, J. W.: Micromechanisms in Particle Hardened Alloys. Cambridge, Cambridge University Press 1980.
- [30] FERRAGUT, R.—SOMOZA, A.—TORRIANI, I.: Mater. Sci. Eng., A334, 2002, p. 1.
[http://dx.doi.org/10.1016/S0921-5093\(01\)01771-3](http://dx.doi.org/10.1016/S0921-5093(01)01771-3)
- [31] MASSARDIER, V.—EPICIER, T.—MERLE, P.: Acta Materialia, 48, 2000, p. 2911.
[http://dx.doi.org/10.1016/S1359-6454\(00\)00085-9](http://dx.doi.org/10.1016/S1359-6454(00)00085-9)
- [32] SIMCHL, A.—DANNINGER, H.—GIERL, C.: Powder Metall., 44, 2001, p. 148.
<http://dx.doi.org/10.1179/003258901666293>

- [33] SIMCHI, A.: *Mater. Design*, 24, 2003, p. 585.
[http://dx.doi.org/10.1016/S0261-3069\(03\)00155-9](http://dx.doi.org/10.1016/S0261-3069(03)00155-9)
- [34] SOLOZHENKO, V. L.—KURAKEVYCH, O. O.: *Solid State Commun.*, 133, 2005, p. 385.
<http://dx.doi.org/10.1016/j.ssc.2004.11.030>
- [35] CASSADA, W. A.—SHIFLET, G. J.—STARKE, E. A., Jr.: *Met. Trans. A*, 22A, 1991, p. 299.
<http://dx.doi.org/10.1007/BF02656799>
- [36] FAHRNER, W. R.: *Handbook of Diamond Technology*. London, Materials Science Foundations 2000.
- [37] RABB, A. R.—ZHENG, X.: *Metall. Trans.*, 22A, 1991, p. 3071.
- [38] CHANG, S. K.: *Mater.Sci. Tech.*, 8, 1992, p. 760.
<http://dx.doi.org/10.1179/026708392790171396>
- [39] DOHERTY, R. D.: *Metal Sci.*, 8, 1974, p. 132.
- [40] HIGGINS, G. T.: *Metal Sci.*, 8, 1974, p. 143.
- [41] HOYT, J. J.: *Acta Metall. Mater.*, 39, 1991, p. 2091.
[http://dx.doi.org/10.1016/0956-7151\(91\)90179-5](http://dx.doi.org/10.1016/0956-7151(91)90179-5)